

LETTER • **OPEN ACCESS**

## Winter cloudiness variability over Northern Eurasia related to the Siberian High during 1966–2010

To cite this article: Alexander Chernokulsky *et al* 2013 *Environ. Res. Lett.* **8** 045012

View the [article online](#) for updates and enhancements.

You may also like

- [Characteristics and mechanisms of the severe compound cold-wet event in southern China during February 2022](#)  
Huixin Li, Bo Sun, Huijun Wang *et al.*
- [On the observed connection between Arctic sea ice and Eurasian snow in relation to the winter North Atlantic Oscillation](#)  
María Santolaria-Otín, Javier García-Serrano, Martín Ménégoz *et al.*
- [Diminishing clear winter skies in Beijing towards a possible future](#)  
Lin Pei and Zhongwei Yan

The Breath Biopsy® Guide  
Fourth edition

FREE

DOWNLOAD THE FREE E-BOOK

BREATH BIOPSY

OWLSTONE MEDICAL

# Winter cloudiness variability over Northern Eurasia related to the Siberian High during 1966–2010

Alexander Chernokulsky<sup>1</sup>, Igor I Mokhov<sup>1</sup> and Natalia Nikitina<sup>1,2</sup>

<sup>1</sup> A M Obukhov Institute of Atmospheric Physics Russian Academy of Sciences, 3, Pyzhevsky, Moscow 119017, Russia

<sup>2</sup> M V Lomonosov Moscow State University, Leninskie Gory, 1, Moscow 119991, Russia

E-mail: [a.chernokulsky@ifaran.ru](mailto:a.chernokulsky@ifaran.ru)

Received 18 July 2013

Accepted for publication 3 September 2013


Published 16 October 2013

Online at [stacks.iop.org/ERL/8/045012](http://stacks.iop.org/ERL/8/045012)

## Abstract

This letter presents an assessment of winter cloudiness variability over Northern Eurasia regions related to the Siberian High intensity (SHI) variations during 1966–2010. An analysis of cloud fraction and the occurrence of different cloud types was carried out based on visual observations from almost 500 Russian meteorological stations. The moonlight criterion was implemented to reduce the uncertainty of night observations. The SHI was defined based on sea-level pressure fields from different reanalyses. We found a statistically significant negative correlation of cloud cover with the SHI over central and southern Siberia and the southern Urals with regression coefficients around 3% hPa<sup>-1</sup> for total cloud fraction (TCF) for particular stations near the Siberian High center. Cross-wavelet analysis of TCF and SHI revealed a long-term relationship between cloudiness and the Siberian High. Generally, the Siberian High intensification by 1 hPa leads to a replacement of one overcast day with one day without clouds, which is associated mainly with a decrease in precipitating and stratiform clouds. These changes point to a positive feedback between cloudiness and the Siberian High.

**Keywords:** Siberian High, winter cloudiness, cloud fraction, cloud types, Northern Eurasia regions

 Online supplementary data available from [stacks.iop.org/ERL/8/045012/mmedia](http://stacks.iop.org/ERL/8/045012/mmedia)

## 1. Introduction

Northern Eurasia has experienced one of the highest rates of surface air temperature (SAT) increase throughout the world in the last decades (Mokhov *et al* 2006, Bulygina *et al* 2007, Jones *et al* 2012). In western Siberia this rate is equal to 1.4 K/century for the last 130 years and 3.2 K/century for the last 50 years (Groisman *et al* 2012). As pointed out by Gong and Ho (2002), the major part of the positive trend of

winter SAT in Northern Eurasia (NE) in the second part of the 20th century can be explained by changes in circulation patterns, including variability of the Siberian High (SH). This atmospheric center of action is a dominant force of winter climate variability in NE. The SH sufficiently influences SAT over the central and eastern part of Asia (Mokhov and Petukhov 1999, Cohen *et al* 2001, Gong and Ho 2002, Mokhov and Khon 2005, Mokhov *et al* 2005, Panagiotopoulos *et al* 2005) and is coherent with the East Asian winter monsoon (Wu and Wang 2002). Paleorecords show that the SH was more intense in a cold climate (during the Little Ice Age) and weaker in a warm one (in the Medieval Warm Period) (Meeker and Mayewski 2002, D'Arrigo *et al* 2005).



Content from this work may be used under the terms of the [Creative Commons Attribution 3.0 licence](http://creativecommons.org/licenses/by/3.0/). Any further distribution of this work must maintain attribution to the author(s) and the title of the work, journal citation and DOI.

A general weakening of the SH is expected in the 21st century due to global warming (Khon and Mokhov 2006, Jeong *et al* 2011). At the same time, the nonlinearity of SH changes is revealed. Particularly, the substantial decrease of SH intensity at the end of the 20th century (Panagiotopoulos *et al* 2005, D'Arrigo *et al* 2005) was replaced with fast recovery in the first decade of the 21st century (Jeong *et al* 2011).

The SH is formed in autumn over the continent due to radiative cooling of the lowest atmospheric layer, which in its turn produces divergence and strengthens high pressure in the central part of Eurasia (Cohen and Entekhabi 1999). The SH reaches its maximum in winter and persists until the middle of spring. It acts as an effective heat sink in the lower troposphere during boreal winter with a  $3 \text{ K d}^{-1}$  cooling rate near its center (Ding and Krishnamurti 1987). Significant contribution to the radiative balance in the SH region is associated with clouds (Ding and Krishnamurti 1987, Kharyutkina *et al* 2012). During the boreal winter, net cloud radiative forcing is positive (Harrison *et al* 1990) and clouds tend to warm the surface (Groisman *et al* 2000). Clouds and cyclonic/anticyclonic activity in the mid-latitudes are closely related to each other (Mokhov *et al* 1992, Tselioudis *et al* 2000, Mokhov *et al* 2009). Cyclonic regimes are associated with bigger cloud fraction while less cloud fraction is observed under anticyclonic conditions. However, a relationship between the SH and cloudiness characteristics has not been investigated in detail in previous studies. An additional argument for such an analysis is higher robustness of sea-level pressure (SLP) as a variable in models and reanalyses compared to clouds which are the major sources of model uncertainties (Bony *et al* 2006, Clement *et al* 2009). Consequently, the ascertainment of a quantitative relationship between clouds and the SH as the key SLP pattern in NE during winter can lead to a better understanding and diagnosis of the evolution of winter cloudiness in this region.

In this letter we present an assessment of cloud cover variability over NE related to the SH variability during 1966–2010. We used reanalysis data for SH intensity detection. Surface visual observations from Russian meteorological stations were used to obtain cloudiness characteristics. Datasets are described in full in section 2 of this letter, section 3 presents the results of the analysis and section 4 concludes the letter.

## 2. Data

Monthly means for SLP from NCEP/NCAR (The National Centers for Atmospheric Prediction/the National Center for Atmospheric Research) reanalysis (Kistler *et al* 2001) were used to characterize SH variability for the 1966–2010 period. We defined the Siberian High intensity (SHI) in two distinct ways. First, the SHI was characterized as the area-averages SLP (hereafter SHIa). Following Panagiotopoulos *et al* (2005) and Jeong *et al* (2011), we averaged SLP winter means over the central part of NE between  $80^{\circ}$ – $120^{\circ}$ E and  $40^{\circ}$ – $65^{\circ}$ N where the SH dominates during the boreal winter. The winter season refers to calendar months from the last December to the present January and February. According

to another definition, the SHI was characterized by the maximal pressure of winter-mean SLP in the aforementioned region (hereafter SHIm) (Mokhov and Khon 2005, Khon and Mokhov 2006). An additional reason to use SHIm together with SHIa is to avoid the NCEP/NCAR SLP inhomogeneity which occurs over the eastern regions of Asia (mostly over China) before late 1970s due to changes in the observational network (Wu *et al* 2005). Because of possible systematic biases of the NCEP/NCAR SLP data (Wu *et al* 2005), we additionally used SLP fields from European reanalysis ERA-Interim (Dee *et al* 2011) (for 1980–2010) and from NOAA-CIRES 20CR reanalysis (National Oceanic and Atmospheric Administration—Cooperative Institute for Research in Environmental Sciences (NOAA-CIRES) 20th Century Reanalysis) (Compo *et al* 2011) (for 1966–2010).

Cloudiness characteristics were obtained from routine 3-hourly observations on Russian meteorological stations, which are collected and subjected to automated quality control at the All-Russian Research Institute of Hydrometeorological Information—World Data Center (RIHMI-WDC) (Razuvaev *et al* 1995). We used data from 493 stations for the 45-year period (1966–2010). The detailed processing of cloudiness information from the RIHMI-WDC dataset was described in full by Chernokulsky *et al* (2011). In brief, this dataset provides information about total and low-level cloud fraction in tenths (TCF and LCF respectively) and about different cloud types from 3-hourly visual observations. The definition of morphological cloud types follows the World Meteorological Organization (WMO) definition except for the nimbostratus clouds that are referred to the low level in RIHMI-WDC archive (but not to the middle one as suggested by the WMO). We recalculated 3-hourly data for TCF and LCF to their winter means by using simple averaging and present it as a percentage. Some stations have sporadic observational gaps. These gaps have a somewhat uniform distribution in time and do not depend on the observational time, so we did not apply any averaging weights to obtain the seasonal means. In addition, we calculated the occurrence of reports with certain amount of clouds and with certain cloud morphological type. Because of possible observer-related uncertainties, we calculated the occurrence for four broad ranges of cloud fraction: for clear sky ( $\text{TCF} < 0.1$ ), for scattered ( $0.1 \leq \text{TCF} \leq 0.5$ ) and broken clouds ( $0.5 < \text{TCF} \leq 0.9$ ) and for overcast conditions ( $\text{TCF} > 0.9$ ). The winter percentage of the cloud type/fraction occurrence is defined as the ratio of the number of reports with a given cloud type/fraction to the total number of reports. We assumed that clouds of different layers are randomly overlapped (Hahn and Warren 2003, Chernokulsky and Eliseev 2013) to obtain the occurrence of high- and middle-level clouds that are obscured by low-level cloudiness. It should be noted here that for many reports different cloud types were observed simultaneously, so the quantitative contribution of different cloud types to TCF is difficult to assess.

To reduce the uncertainty of night observations due to inappropriate illumination of clouds, we additionally analyzed cloud data which meet the moonlight criterion suggested by Hahn *et al* (1995). This criterion filters out observations that

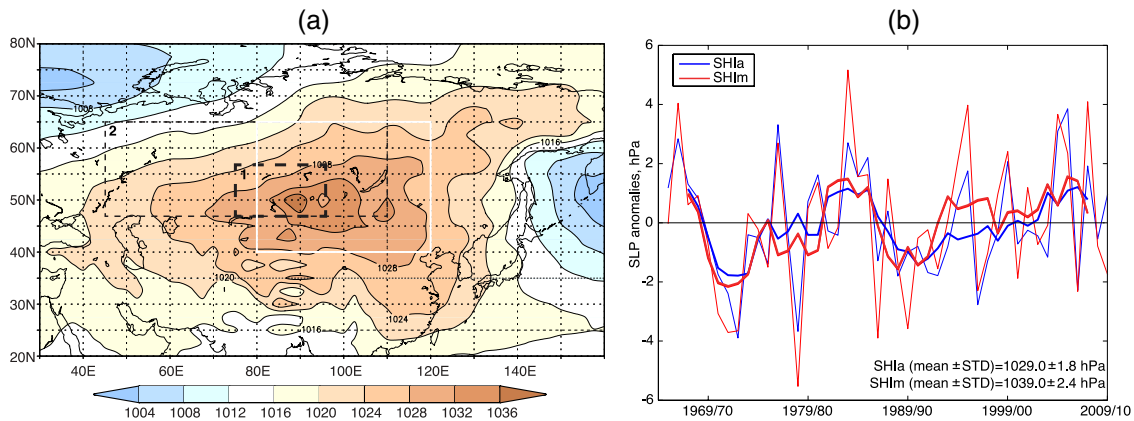


**Figure 1.** Mean winter sea-level pressure during the period 1966–2010 (a) and interannual variability of SHIa and SHIm (thin lines) with 5-year running averaged values (thick lines) (b) based on NCEP/NCAR reanalysis. White box in (a) corresponds to SHIa region. Regions 1 and 2 are delineated in (a) by black dashed lines (see figure 5 and text below for further details).

were made during dark nights. Particularly, the threshold for the sun angle was  $9^\circ$  below the horizon and the threshold for the relative lunar illuminance (which takes into account the phase and the height of the moon) was 0.11 (Hahn *et al* 1995). About 40% of all winter observations in the southern regions of Russia and about 60% in the northern regions were excluded after the implementation of this criterion. We present the analysis of the original dataset as well to avoid a possible exclusion of the part of cloudiness natural variability because of the implementation of the moonlight criterion.

### 3. Results

#### 3.1. Interannual variability of the Siberian High intensity

The Siberian High is a prominent pattern of the winter SLP field which covers most of Eurasia. The 1020 hPa contour for mean winter SLP field reaches the Black Sea in the west and Chukotka in the east (figure 1(a)). In the south, the SH propagates to the east-southern regions of China and it is responsible for cold surges over China (Qian *et al* 2001). The location of the maximum SLP has little variation in time. Among 45 years of analysis, 40 times the maximum of the SH located at  $50^\circ\text{N}$  and  $90^\circ\text{E}$ , 4 times it located at  $50^\circ\text{N}$  and  $87.5^\circ\text{E}$  and only once was its location at  $52.5^\circ\text{N}$  and  $100^\circ\text{E}$ . Mokhov and Khon (2005) showed that the SH center can shift west-southward during the Northern Hemisphere warming based on observations, while NCEP/NCAR reanalysis data do not confirm this tendency.

The interannual variability of the SH is roughly the same for SHIa and SHIm (figure 1(b)). The correlation coefficient between SHIa and SHIm for 1966–2010 is 0.86 with a confidence level higher than 99% based on Student's *t*-test. Means and standard deviations (STD) of SHIa and SHIm for 1966–2010 equal  $1029.0 \pm 1.8$  and  $1039.0 \pm 2.3$  hPa respectively. Anomalies of SHIa and SHIm can reach 4–5 hPa for particular years. Two minima of SHI at the beginning of 1970s and near 1990, and two maxima in the middle of the 1980s and at the end of the 2010s were observed during the analyzed 45-year period. In general, oscillations

of the SHI appeared with period about 15–30 years. Based on paleorecords, this periodicity of the SH activity is distinguished as significant for the last 400 years by Meeker and Mayewski (2002).

Interannual changes of SHI from ERA-Interim and NOAA-CIRES 20CR reanalyses are highly correlated with those from NCEP/NCAR (see supplementary data, figure S1 and table S1, available at [stacks.iop.org/ERL/8/045012/mmedia](http://stacks.iop.org/ERL/8/045012/mmedia)). The correlation coefficients are higher for SHIa (about 0.9–0.95) than for SHIm (about 0.8–0.9). All correlation coefficients are statistically significant at the 99% confidence level. In general, values of SHIa from different reanalyses are distinguished from each other for 1–2 hPa (figure S1), while differences in SHIm values from different reanalyses can reach 3–4 hPa for particular years (not shown).

#### 3.2. Climatology of winter cloudiness over Northern Eurasia

Winter-mean TCF over Russia reaches its maximum in European regions of Russia (ER) (see supplementary, figure S2, available at [stacks.iop.org/ERL/8/045012/mmedia](http://stacks.iop.org/ERL/8/045012/mmedia)). It is up to 80% according to the original data (OD) (figure S2(a)) and up to 85% according to the data with moonlight criterion implementation (DMC) (figure S2(b)). Minimal values of TCF are observed south of the Far East (FE) (down to 30–35% from OD and about 40% from DMC). In Siberia the difference of TCF between DMC and OD exceeded 10% for particular stations. It is about 50–60% according to OD and about 60–70% according to DMC. Winter-mean LCF (figures S2(c) and (d)) is decreasing eastward from 60 to 70% in the western regions of Russia to 5–10% in the eastern regions. One local maximum of LCF is noted over Sakhalin and Kuril Islands. In general, differences of LCF between DMC and OD do not exceed 2–3% for various stations.

High values of winter TCF are associated with the high occurrence of reports with overcast conditions (OvcO) which is about 70% of all reports in ER and about 55–60% in Siberia (figures S3(g) and (h), available at [stacks.iop.org/ERL/8/045012/mmedia](http://stacks.iop.org/ERL/8/045012/mmedia)). OvcO has a minimum south of FE (about 25–35%) where the occurrence of reports with clear



sky (ClrO) reaches its maximum (about 60% from OD and 50% from DMC). ClrO is about 20% in ER and about 30% in Siberia (figures S3(a) and (b)). The occurrence of reports with scattered and broken clouds (SctO and BknO respectively) is about 10–20% in all regions (figures S3(c)–(f)). Higher values of ClrO and OvcO compared to SctO and BknO points to a U-shaped distribution of cloud fraction derived from surface visual observations.

The main common types of cloudiness in winter over Northern Eurasia are high-level cloud types (cirrus, cirrostratus and cirrocumulus). The occurrence of reports with all high-level clouds (CiO) is about 20–40% of all reports in ER and the coastal regions of the FE and is up to 70–90% in the central part of Siberia (figure S4(a), available at [stacks.iop.org/ERL/8/045012/mmedia](http://stacks.iop.org/ERL/8/045012/mmedia)). The occurrence of middle-level cloud types (altostratus and altocumulus, AscO) is about 40–50% for most regions of Russia except the most western part of ER and south of the FE where AscO is about 10–30% (figure S3(b)). Among low-level cloud types, stratus and stratocumulus clouds are the most frequent especially over western regions of ER where LCF reaches its maximum (see figures S2(c) and (d)). The occurrence of stratus and stratocumulus clouds (StscO) is about 40–50% in this region (figure S4(e)) and decreases eastward to 5–15% in south of east Siberia and the FE (where LCF is also small). Because of the cold underlying surface, the occurrence of convective cloud forms (ConvO), which include cumulus and cumulonimbus clouds, does not exceed 20% except in the coastal regions of Barents Sea and the Pacific Ocean where it reaches 50–70% for particular stations (figure S4(c)). The major contribution to ConvO is given by cumulonimbus clouds, which are associated with frontal systems of mid-latitude cyclones. Another type of precipitating cloud is nimbostratus clouds (NbsO) whose occurrence is about 20% for ER and 10% for Siberia and the FE (figure S4(d)). The occurrence of precipitating clouds (cumulonimbus and nimbostratus, PrecO) varies from 30% in RE and south of Siberia to 10% in north of Siberia and the continental part of the FE. In the coastal regions of the FE, PrecO reaches 60–70% for particular stations. In general, the difference between OD and DMC for the occurrence of cloud types does not exceed 2–3% except for CiO and AscO. For the occurrence of these cloud types the difference between OD and DMC can reach 10% for particular stations.

### 3.3. Variations of cloudiness related to variability of the Siberian High intensity

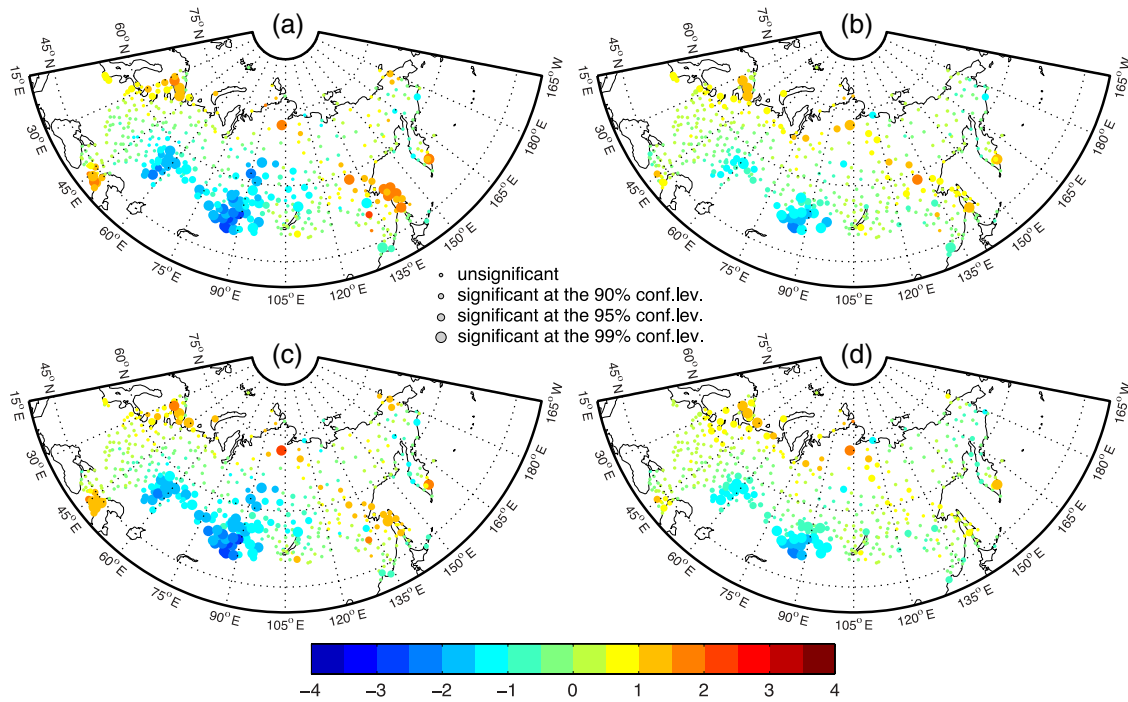
We estimated the relationship between the SHI ( $X$ ) and cloudiness characteristics ( $Y$ ) with the analysis of corresponding coefficients of linear regressions  $k_{\text{regr}}(Y:X)$  for each meteorological station for the period 1966–2010. The statistical significance was determined from Student's  $t$ -test.

Figure 2 presents coefficients of linear regression of TCF to SHI  $k_{\text{regr}}(\text{TCF:SHI})$  from NCEP/NCAR reanalysis. In general, an intensification of the SH leads to a decrease in cloudiness in the central part of the SH and to the west from it. TCF correlates negatively with SHIa (figure 2(a))

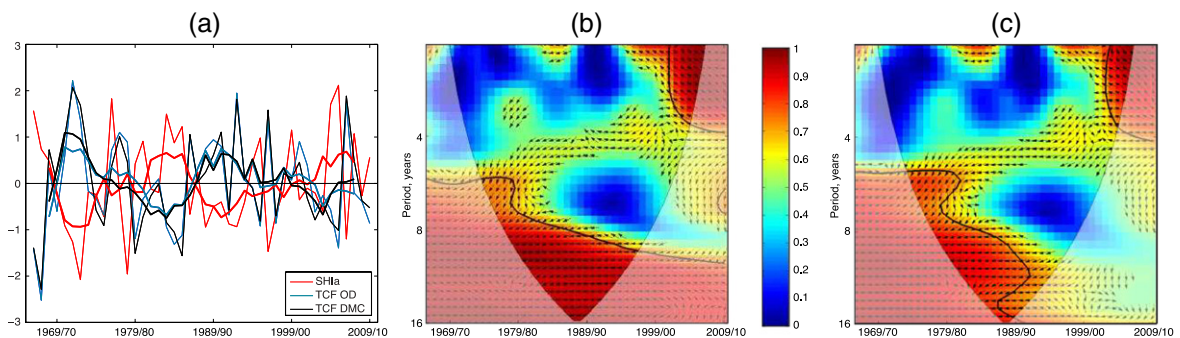
in vast regions of central and southern Siberia and the Urals—a statistically significant negative correlation is noted for stations from 55 to 110°E and from 47 to 65°N. For the SH central part  $k_{\text{regr}}(\text{TCF:SHIa})$  is close to  $-3\% \text{ hPa}^{-1}$  with the correlation coefficient more than  $-0.6$ . Presumably, negative correlation of TCF and SHI locates also in the northern part of Kazakhstan but additional data are required to confirm this point. The influence of SHIm on TCF (figures 2(b) and (d)) is qualitatively close to that for SHIa but its effect is more localized. Negative correlation of TCF with SHIm appeared mostly close to the SH center and values of  $k_{\text{regr}}(\text{TCF:SHIm})$  were lower by  $1\text{--}2\% \text{ hPa}^{-1}$  than  $k_{\text{regr}}(\text{TCF:SHIa})$ . The signal of SHI in winter cloudiness variability is robust to the moonlight criterion implementation except for particular stations on Sakhalin Island, where  $k_{\text{regr}}(\text{TCF}_{\text{DMC}}:\text{SHI})$  has less positive values than  $k_{\text{regr}}(\text{TCF}_{\text{OD}}:\text{SHI})$  (figure 2). Similar findings were obtained based on ERA-Interim and NOAA-CIRES 20CR SLP (see figure S5, available at [stacks.iop.org/ERL/8/045012/mmedia](http://stacks.iop.org/ERL/8/045012/mmedia)), which point to the robustness of our results to the SLP data choice.

Figure 3(a) presents the interannual variability of SHIa and TCF from OD and DMC for the meteorological station Zmeinogorsk, which is located near the center of the SH and has the highest absolute value of the correlation coefficient of TCF and SHI among other stations (it is  $-0.63$  for TCF from DMC and SHIa). It is clearly seen that periods with high SH intensity coincide with periods of low values of TCF and vice versa. Particularly, TCF has maxima in the beginning of 1970s and near 1990, which corresponds to SHI minima (see also figure 1(b)). During recent decades, TCF slightly decreased, which was also found by Chernokulsky *et al* (2011). Similar TCF variability is noted for other weather stations in southern and central Siberia and the Urals (not shown). Cross-wavelet analysis of TCF at Zmeinogorsk and SHIa (figures 3(b) and (c)) elucidated the presence of a long-term statistically significant negative relationship between TCF and SHIa. Short-term coherence appeared only for the last decade.

A decrease of TCF because of SH intensification comes from changes in the TCF distribution, particularly from a decrease of OvcO (figure 4(b)), and an increase of ClrO (figure 4(a)) in the aforementioned region ( $k_{\text{regr}}(\text{OvcO}_{\text{DMC}}:\text{SHIa})$  is down to  $-3\%$  of all reports per 1 hPa and  $k_{\text{regr}}(\text{ClrO}_{\text{DMC}}:\text{SHIa})$  is up to 2.5%). Positive correlation between SHI and SctO was also revealed (up to  $1\% \text{ hPa}^{-1}$ ) (figure S6(a), available at [stacks.iop.org/ERL/8/045012/mmedia](http://stacks.iop.org/ERL/8/045012/mmedia)). In general, the occurrence of reports with broken clouds does not depend on SHI (figure S6(b)). Similar findings were made for ERA-Interim and NOAA-CIRES 20CR SLP data (figure S7, available at [stacks.iop.org/ERL/8/045012/mmedia](http://stacks.iop.org/ERL/8/045012/mmedia)). Redistribution between clear sky and overcast reports is noted as for individual stations and for wide regions. We analyzed the differences of the occurrence of reports with various TCF ( $\Delta\text{OvcO}$ ,  $\Delta\text{SctO}$ ,  $\Delta\text{BknO}$  and  $\Delta\text{ClrO}$ ) between 10 years with the highest values of SHIa and 10 years with the lowest ones (table 1) for two regions: (1) south of West Siberia (47°–57°N, 75°–95°E, region 1) and (2) south and center of the Urals and Siberia (47°–65°N,



**Figure 2.** Coefficient of linear regression ( $\% \text{ hPa}^{-1}$ ) of TCF from OD ((a) and (b)) or from DMC ((c) and (d)) to SHIa ((a) and (c)) or SHIm ((b) and (d)) from NCEP/NCAR reanalysis. The size of the circles corresponds to the confidence level of statistical significance (90, 95 and 99%).



**Figure 3.** Interannual variability of SHIa (based on NCEP/NCAR reanalysis) and TCF (anomalies normalized on STD) at the meteorological station Zmeinogorsk ( $51.15^{\circ}\text{N}$ ,  $82.2^{\circ}\text{E}$ ) and 5-year running averaged time series (thick lines) (a), and cross-wavelet coherence between SHIa and TCF from OD (b) and DMC (c) for this station. Following Grinsted *et al* (2004) the 95% confidence level against red noise is shown in (b), (c) as a thick contour. The relative phase relationship is shown as arrows (with in-phase pointing right, anti-phase pointing left, and SHI leads TCF by  $90^{\circ}$  pointing straight down).

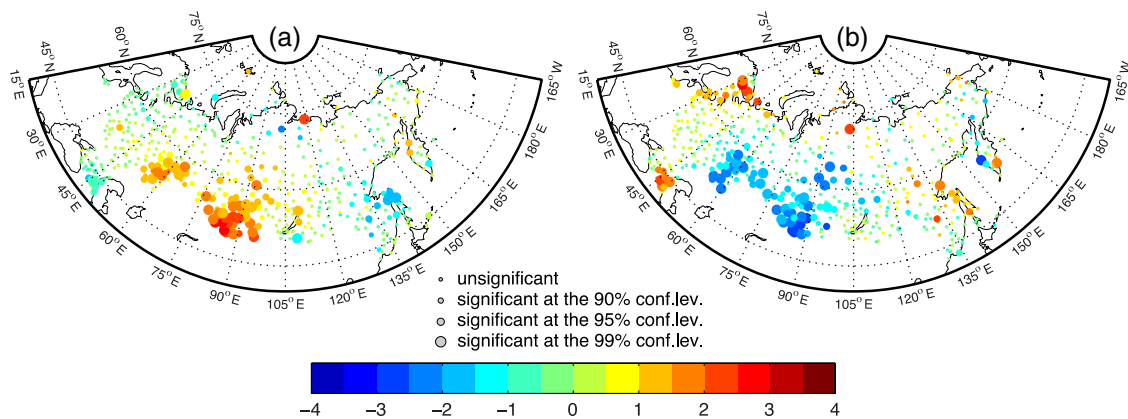


**Figure 4.** The same as figure 2 but for ClrO (a) and OvCo (b) from DMC and SHIa from NCEP/NCAR reanalysis.

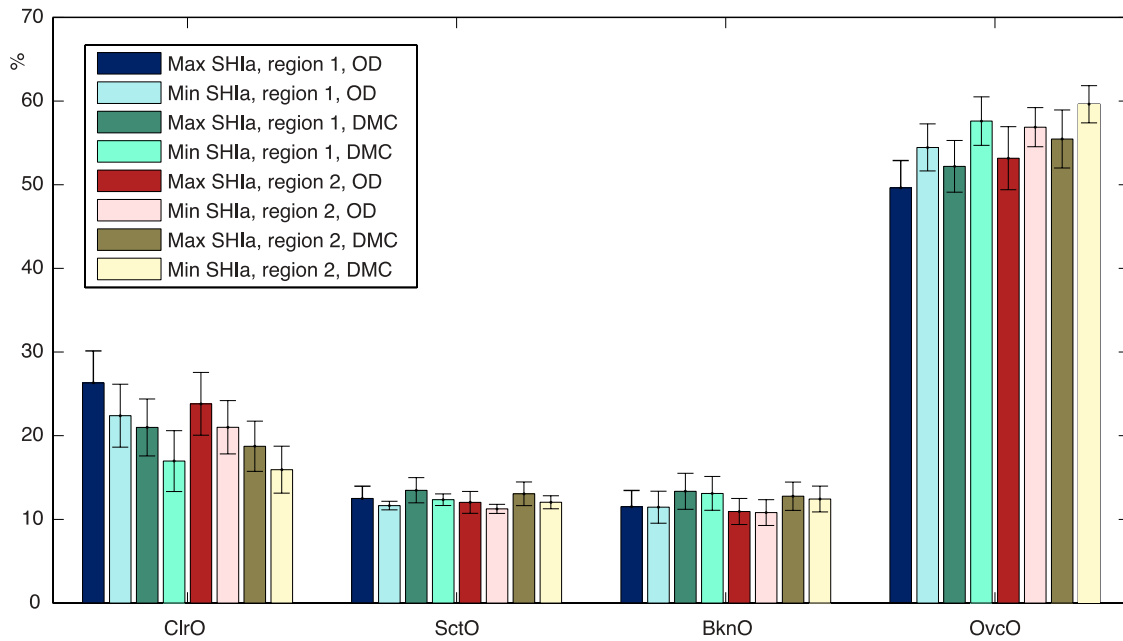


**Figure 5.** The difference (mean and standard deviation) of ClrO, SctO, BknO and OvcO between 10 years with the maximum (dark colors) and 10 years with the minimum (light colors) of SHIa for two region: 47°–57°N, 75°–95°E (region 1) and 47°–65°N, 45°–110°E (region 2) (delineated in figure 1(a)).

**Table 1.** Winters with the highest/lowest values of SHIa (with mean and standard deviation).

Winters	Mean and STD of SHIa (hPa)
Winters with the maximal SHIa 1966/67, 1976/77, 1980/81, 1983/84, 1985/86, 1995/96, 1999/00, 2004/05, 2005/06, 2007/08	1031.54 ± 0.74
Winters with the minimal SHIa 1970/71, 1971/72, 1972/73, 1975/76, 1978/79, 1988/89, 1991/92, 1992/93, 1996/97, 2006/07	1026.66 ± 0.86

45°–110°E, region 2). Figure 5 shows the results of this composite analysis. The major changes are observed for clear sky reports and reports with overcast conditions. The difference between years with maximal and minimal SHIa is more prominent for region 1 from DMC reports:  $\Delta\text{ClrO}$  is equal to 4% (with STD close to 3.5%) and  $\Delta\text{OvcO}$  is equal to 5.4% (with STD close to 3%). The sensitivity of cloudiness differences to SHIa differences can be estimated by the ratios  $\Delta\text{ClrO}/\Delta\text{SHIa}$  and  $\Delta\text{OvcO}/\Delta\text{SHIa}$  (table 2). It should be noted that these differences are statistically insignificant.

The major changes are connected with the changes in middle-level clouds. AscO decreases at the southern and central parts of Siberia and the Urals by 2–3%  $\text{hPa}^{-1}$  SHIa (figure 6(a)) mostly because of the decrease in altostratus occurrence with SH intensification. Low-level stratiform cloudiness has a negative correlation with the SHI at the same region as well (figures S8(c) and (d), available at [stacks.iop.org/ERL/8/045012/mmedia](http://stacks.iop.org/ERL/8/045012/mmedia)). In addition, stratus and stratocumulus clouds become more infrequent over most regions of ER with an intensification of the SH. They are replaced here with high-level clouds (figure S8(a)), which tend to increase in ER with SH intensification. Convective cloudiness decreases over most of Russia except Sakhalin Island with an increase of SHI (figure S8(b)). A negative correlation of ConvO and NbsO with SHI leads to a negative

**Table 2.**  $\Delta\text{ClrO}/\Delta\text{SHIa}$  and  $\Delta\text{OvcO}/\Delta\text{SHIa}$  for different regions and cloud datasets (%  $\text{hPa}^{-1}$ ).

	Original cloud dataset		Cloud dataset with moonlight criterion	
	Region 1	Region 2	Region 1	Region 2
$\Delta\text{ClrO}/\Delta\text{SHIa}$	0.8	0.57	0.82	0.57
$\Delta\text{OvcO}/\Delta\text{SHIa}$	−0.99	−0.76	−1.11	−0.85

correlation between PrecO and SHI (figure 6(b)). Thus, an intensification of the SH results in a decrease of winter precipitation in vast regions of NE (see figure S9 for details, available at [stacks.iop.org/ERL/8/045012/mmedia](http://stacks.iop.org/ERL/8/045012/mmedia)).

A positive correlation between TCF and SHI is localized in the coastal regions of Barents and Okhotsk Seas, Northern Siberia, and Caucasus, where  $k_{\text{reg}}$  (TCF:SHIa) can reach 1–2%  $\text{hPa}^{-1}$  for particular stations. These changes in cloudiness indicate changes in circulation regimes. Due to an intensification of the SH, Atlantic stormtracks can be shifted to the north (to the Barents Sea and northern Siberia) or to the south (Caucasus). Cyclones which are formed over the Pacific Ocean cannot propagate far into the continent because of the intense SH, which leads to an increase in TCF over the south-western part of the Okhotsk Sea.

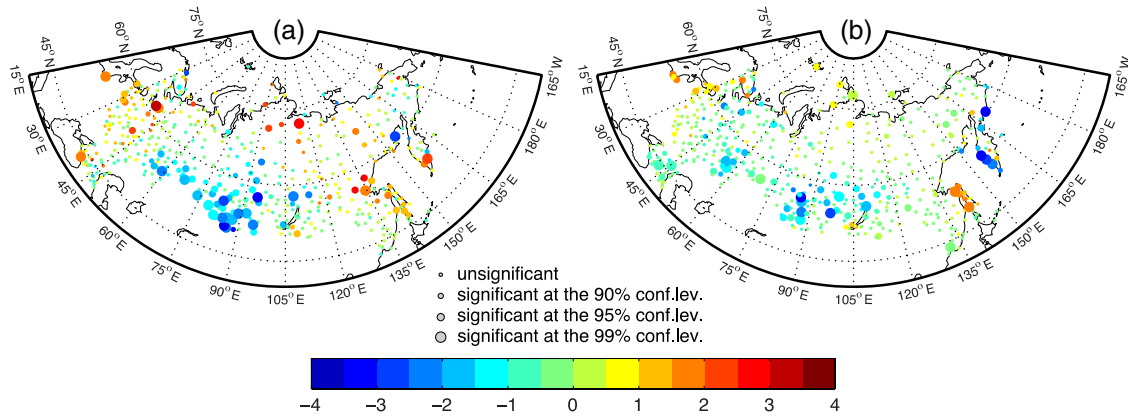


**Figure 6.** The same as figure 2 but for AscO (a) and PrecO (b) from DMC and SHIa from NCEP/NCAR reanalysis.

#### 4. Discussion and conclusions

In this letter we presented a quantitative assessment of the relationship between the SH and winter cloudiness characteristics in NE during the last 45 years. We found a statistically significant negative correlation of cloud cover with SHI variability in vast regions of central and southern Siberia and the southern Urals. The corresponding regression coefficient reaches almost 3% of TCF per hPa for particular stations near the center of the SH. Cross-wavelet analysis of TCF and the SHI revealed a long-term relationship between winter cloudiness and the SH. In general, a decrease of TCF comes from a decrease of overcast reports and an increase of clear sky reports. The regression coefficient for the clear sky reports occurrence is about 2–3% from all reports per 1 hPa for stations near the SH center. The same values are obtained for the overcast reports occurrence but with a negative sign. Roughly, SH intensification by 1 hPa can lead to a replacement of 2–3 overcast days with 2–3 days without clouds during the whole winter for stations near the SH center. For the entire Urals and western Siberia the sensitivity of clear/overcast days to SHI is 2–3 times less. An increase in SHI during the last decade leads to a decrease in winter cloudiness over Siberia and the Urals. This decrease in winter cloudiness was noted by Chernokulsky *et al* (2011). It was also shown that TCF tends to increase over NE during other seasons (Sun *et al* 2001, Chernokulsky *et al* 2011). According to our results this decrease in winter cloudiness is associated with the strengthening of the SH. These results are robust to the SLP data choice.

It is suggested that the strengthening of the anticyclonic activity over NE in the last decade can be one of the reasons for an increase in cold winter occurrence at the beginning of the 21st century in NE (Zhang *et al* 2012). We suggest that cloudiness changes should attract more attention. Cloud effects on temperature (temperature difference between average and clear sky conditions) can reach 4–8 K in NE regions during winter (Groisman *et al* 2000). We found that a negative correlation of TCF with SHI is mostly associated with a decrease of stratocumulus, stratus and altostratus cloud occurrences. According to Chen *et al* (2000), these stratiform

cloud types have significant influence on surface downward longwave fluxes. Thus, changes in cloudiness related to the SH variability can sufficiently influence SAT. Further analysis should be carried out to assess the radiative effects of cloudiness variations related to SHI changes. However, the observational data for this kind of analysis should be used with caution due to large discrepancies among datasets in the high latitudes during the boreal winter (Chernokulsky and Mokhov 2012). It is also worth noting that a negative correlation between cloudiness characteristics and SHI in the central part of the SH points to a positive feedback between SLP and cloudiness changes. An increase of SLP leads to a decrease of clouds under anticyclonic conditions, which in turn leads to an intensification of radiative cooling and further strengthening of the SH. The optically thick clouds over Northern Eurasia in winter can postpone the SH formation because of prevention of radiative cooling. An additional analysis on a daily timescale basis is needed for a quantitative assessment of such effects.

In the Arctic regions, FE coastal regions and the Caucasus, SH intensification is associated with an increase in cloudiness mostly due to an increase in the occurrence of low-level clouds. Here, the influence of other atmospheric centers of action (Aleutian Low, Icelandic Low, Azores High) as well as circulation indices like Arctic Oscillation or North Atlantic Oscillation (NAO) on cloudiness should be taken into account. In particular, winter TCF over NE has a statistically significant correlation with NAO (positive in western Russian regions and negative in eastern regions; see figure S10, available at [stacks.iop.org/ERL/8/045012/mmedia](http://stacks.iop.org/ERL/8/045012/mmedia)). However, this connection is relatively weak in the south of Siberia where the SH influence is the strongest. Thus, a comprehensive assessment of the joint influence of major components of the Northern Hemisphere climate system on winter cloudiness over NE and its radiative impact can give important additional information on recent regional climate variations in Northern Eurasia.

#### Acknowledgments

We are grateful to Vyacheslav Khon and Vladimir Semenov for fruitful discussions and two anonymous reviewers



for thoughtful comments. We thank Ryan Eastman for providing the routine for computing the moonlight criterion. The RIHMI-WDC data were obtained from [www.meteo.ru](http://www.meteo.ru) web-site. The NCEP/NCAR data are from the Research Data Archive (RDA), which is maintained by CISL at NCAR. Support for this research was provided by the Grants of the RF President (MK-3259.2012.5 and NSh-5467.2012.5), by Russian Ministry of Education and Science under contracts 14.740.11.1043 and 8617, by the Russian Foundation for Basic Research under Grants 11-05-01139, 11-05-00579 and 12-05-00972, and by programs of The Russian Academy of Sciences.

## References

- Bony S *et al* 2006 How well do we understand and evaluate climate change feedback processes? *J. Clim.* **19** 3445–82
- Bulygina O N, Razuvaev V N, Korshunova N N and Groisman P Y 2007 Climate variations and changes in extreme climate events in Russia *Environ. Res. Lett.* **2** 045020
- Chen T, Rossow W B and Zhang Y 2000 Radiative effects of cloud-type variations *J. Clim.* **13** 264–86
- Chernokulsky A V, Bulygina O N and Mokhov I I 2011 Recent variations of cloudiness over Russia from surface daytime observations *Environ. Res. Lett.* **6** 035202
- Chernokulsky A V and Eliseev A V 2013 Climatology of satellite-derived cloud overlap parameter *Research Activities in Atmospheric and Oceanic Modelling* vol 43, ed A Zadra (Geneva: World Meteorological Organization) pp 2.03–5
- Chernokulsky A V and Mokhov I I 2012 Climatology of total cloudiness in the Arctic: an intercomparison of observations and reanalyses *Adv. Meteorol.* **2012** 542093
- Clement A C, Burgman R and Norris J R 2009 Observational and model evidence for positive low-level cloud feedback *Science* **235** 460–4
- Cohen J and Entekhabi D 1999 Eurasian snow cover variability and Northern Hemisphere climate predictability *Geophys. Res. Lett.* **26** 345–8
- Cohen J, Saito K and Entekhabi D 2001 The role of the Siberian high in Northern Hemisphere climate variability *Geophys. Res. Lett.* **28** 299–302
- Compo G P *et al* 2011 The twentieth century reanalysis project *Q. J. R. Meteorol. Soc.* **137** 1–28
- D'Arrigo R, Jacoby G, Wilson R and Panagiotopoulos F 2005 A reconstructed Siberian High index since A D 1599 from Eurasian and North American tree rings *Geophys. Res. Lett.* **32** L05705
- Dee D P *et al* 2011 The ERA-Interim reanalysis: configuration and performance of the data assimilation system *Q. J. R. Meteorol. Soc.* **137** 553–97
- Ding Y and Krishnamurti T N 1987 Heat budget of the Siberian High and winter monsoon *Mon. Weather Rev.* **115** 2428–49
- Gong D Y and Ho C H 2002 The Siberian High and climate change over middle to high latitude Asia *Theor. Appl. Climatol.* **72** 1–9
- Grinsted A, Moore J C and Jevrejeva S 2004 Application of the cross wavelet transform and wavelet coherence to geophysical time series *Nonlinear Process. Geophys.* **11** 561–6
- Groisman P Y, Bradley R S and Sun B 2000 The relationship of cloud cover to near-surface temperature and humidity: comparison of GCM simulations with empirical data *J. Clim.* **13** 1858–78
- Groisman P Y *et al* 2012 Climate changes in Siberia *Regional Environmental Changes in Siberia and their Global Consequences* ed P Y Groisman and G Gutman (Dordrecht: Springer) pp 57–109
- Hahn C J and Warren S G 2003 *A Gridded Climatology of Clouds Over Land (1971–96) and Ocean (1954–97) from Surface Observations Worldwide (NDP-026E)* (Oak Ridge, TN: Carbon Dioxide Information Analysis Center)
- Hahn C J, Warren S G and London J 1995 The effect of moonlight on observation of cloud cover at night, and application to cloud climatology *J. Clim.* **8** 1429–46
- Harrison E F, Minnis P, Barkstrom B R, Ramanathan V, Cess R D and Gibson G G 1990 Seasonal variation of cloud radiative forcing derived from the Earth radiation budget experiment *J. Geophys. Res.* **95** 18687–703
- Jeong J-H, Ou T, Linderholm H W, Kim B-M, Kim S-J, Kug J-S and Chen D 2011 Recent recovery of the Siberian High intensity *J. Geophys. Res.* **116** D23102
- Jones P D, Lister D H, Osborn T J, Harpham C, Salmon M and Morice C P 2012 Hemispheric and large-scale land-surface air temperature variations: an extensive revision and an update to 2010 *J. Geophys. Res.* **117** D05127
- Kharyutkina E V, Ippolitov I I and Loginov S V 2012 The variability of radiative balance elements and air temperature over the Asian region of Russia *Biogeosciences* **9** 1113–23
- Khon V C and Mokhov I I 2006 Model estimates for the sensitivity of atmospheric centers of action to global climate changes *Izv. Atmos. Ocean. Phys.* **42** 688–95
- Kistler R *et al* 2001 The NCEP–NCAR 50-year reanalysis: monthly means CD-ROM and documentation *Bull. Am. Meteorol. Soc.* **82** 247–68
- Meeker L D and Mayewski P A 2002 A 1400-year high-resolution record of atmospheric circulation over the North Atlantic and Asia *Holocene* **12** 257–66
- Mokhov I I, Chernokul'skii A V, Akperov M G, Dufresne J-L and Le Treut H 2009 Variations in the characteristics of cyclonic activity and cloudiness in the atmosphere of extratropical latitudes of the Northern Hemisphere based from model calculations compared with the data of the reanalysis and satellite data *Dokl. Earth Sci.* **424** 147–50
- Mokhov I I, Eliseev A V, Demchenko P F, Khon V C, Akperov M G, Arzhanov M M, Karpenko A A, Tikhonov V A, Chernokulsky A V and Sigaeva E V 2005 Climate changes and their assessment based on the IAP RAS global model simulations *Dokl. Earth Sci.* **402** 591–5
- Mokhov I I, Karpenko A A and Stott P A 2006 Highest rates of regional climate warming over the last decades and assessment of the role of natural and anthropogenic factors *Dokl. Earth Sci.* **406** 158–62
- Mokhov I I and Khon V Ch 2005 Interannual variability and long-term tendencies of change in atmospheric centers of action in the Northern Hemisphere: analyses of observational data *Izv. Atmos. Ocean. Phys.* **41** 657–66
- Mokhov I I, Mokhov O I, Petukhov V K and Khairullin R R 1992 On the influence of cloudiness on vortex activity in the atmosphere during climate change *Russ. Meteorol. Hydrol.* **17** 5–11
- Mokhov I I and Petukhov V K 1999 Atmospheric centers of action and tendencies of their change *Izv. Atmos. Ocean. Phys.* **36** 292–9
- Panagiotopoulos F, Shahgedanova M, Hannachi A and Stephenson D B 2005 Observed trends and teleconnections of the Siberian High: a recently declining center of action *J. Clim.* **18** 1411–22
- Qian W, Zhang H, Zhu Y and Lee D-K 2001 Interannual and interdecadal variability of East Asian ACAs and their impact on temperature of China in winter season for the last century *Adv. Atmos. Sci.* **18** 511–23
- Razuvaev V N, Apasova E G and Martuganov R A 1995 *Six- and Three-Hourly Meteorological Observation from 223 USSR Stations (NDP-048)* (Oak Ridge, TN: Carbon Dioxide Information Analysis Center) plus appendixes

- Sun B, Groisman P Y and Mikhov I I 2001 Recent changes in cloud-type frequency and inferred increases in convection over the United States and the former USSR *J. Clim.* **14** 1864–80
- Tselioudis G, Zhang Y and Rossow W B 2000 Cloud and radiation variations associated with northern midlatitude low and high sea level pressure regimes *J. Clim.* **13** 312–27
- Wu R, Kinter J L III and Kirtman B P 2005 Discrepancy of interdecadal changes in the Asian region among the NCEP–NCAR reanalysis, objective analyses, and observations *J. Clim.* **18** 3048–67
- Wu B and Wang J 2002 Winter Arctic oscillation, Siberian High and East Asian winter monsoon *Geophys. Res. Lett.* **29** 1897
- Zhang X, Lu C and Guan Z 2012 Weakened cyclones, intensified anticyclones and recent extreme cold winter weather events in Eurasia *Environ. Res. Lett.* **7** 044044